

Discontinuous transition of molecular-hydrogen chain to the quasi-atomic state: Exact diagonalization – ab initio approach

Andrzej P. Kądziaława,^{1,*} Andrzej Biborski,^{2,†} and Józef Spałek^{1,2,‡}

¹*Marian Smoluchowski Institute of Physics, Jagiellonian University,
ulica Łojasiewicza 11, PL-30-348 Kraków, Poland*

²*Academic Centre for Materials and Nanotechnology,
AGH University of Science and Technology, al. Mickiewicza 30, PL-30-059 Kraków, Poland*

(Dated: October 5, 2018)

We obtain in a direct and rigorous manner a transition from a stable molecular hydrogen nH_2 single chain to the quasiautomic two-chain $2nH$ state. We devise an original method composed of an exact diagonalization in the Fock space combined with an ab initio adjustment of the single-particle wave function in the correlated state. In this approach the well-known problem of double-counting the interparticle interaction does not arise at all. The transition is strongly discontinuous, and appears even for relatively short chains possible to tackle, $n = 3 \div 6$. The signature of the transition as a function of applied force is a discontinuous change of the equilibrium intramolecular distance. The corresponding change of the Hubbard ratio U/W reflects the Mott–Hubbard-transition aspect of the atomization. Universal feature of the transition relation to the Mott criterion for the insulator–metal transition is also noted. The role of the electron correlations is thus shown to be of fundamental significance in this case. The long-range nature of Coulomb interactions is included.

PACS numbers: 31.15.A-, 71.27.+a, 67.80.F-, 67.63.Gh

1. Motivation The metallization of solid hydrogen is one of the central problems in physics [1–4], as well as in astrophysics of Jupiter, Saturn, and exoplanets [5]. The building block, the H_2 molecule, is relatively simple, since the electrons are in the spin-singlet state in the ground state composed mainly of $1s$ states of atoms. Those molecular states with the experimental value of bond length $R \approx 1.401a_0$ [6] form at ambient pressure a molecular crystal with the lattice constant $a \sim 7a_0 \gg R$ [7], where a_0 is the Bohr radius. Thus, to achieve atomic structure and metallicity one has to break the molecular bond, e.g., by achieving a more typical atomic solid configuration with $a \sim R$, what amounts in practice to applying an enormous pressure, as demonstrated repeatedly over the decades [2, 8]. But even then one may not achieve metallicity, as due to the relatively large atomic separation the system may compose a Mott (or Mott–Hubbard) insulator [9, 10], as the original interelectronic correlation effects may still be sufficiently strong. The fundamental aspect of this paper is to address this issue in a rigorous manner, as detailed below.

The related and probably more intriguing question related to the hydrogen metallization is the conjecture that the system may exhibit a room-temperature superconductivity. The line of reasoning [11, 12] is based on the Bardeen-Cooper-Schrieffer (BCS) theory that as the critical temperature T_s is proportional to $M^{-1/2}$, where M is the ionic mass, then the hydrogen metal should have T_s at least one order of magnitude higher than that of a typical metal. However, here again the correlation ef-

fects must be carefully taken into account as they should not be too strong to destroy the metallicity, but essential, as they can lead by themselves also to the high-temperature superconductivity when the starting point is the atomic solid with half-filled Mott–Hubbard metal [13]. A marriage of strong electron–lattice and correlation effects should be accounted for at the starting stage. In this respect, here we determine rigorously the magnitude of the local correlation effects as described by the effective extended Hubbard model at the molecular \rightarrow quasiautomic solid transition. The values of local electron–proton coupling have been calculated elsewhere [14].

Recently, the molecular–atomic hydrogen transition has been discussed by a number of methods [15–18]. In this respect, the present results can be regarded as a basis for testing the approximate methods.

2. Model and method We start with the extended Hubbard model with additional term $V_{\text{ion-ion}}$ expressing ion–ion repulsion namely,

$$\hat{\mathcal{H}} = \sum_i \epsilon_i \hat{n}_i + \sum_{\sigma, i \neq j} t_{ij} \hat{c}_{i\sigma}^\dagger \hat{c}_{j\sigma} + U \sum_i \hat{n}_{i\uparrow} \hat{n}_{i\downarrow} \quad (1)$$

$$+ \frac{1}{2} \sum_{i \neq j} K_{ij} \hat{n}_i \hat{n}_j + V_{\text{ion-ion}},$$

where ϵ_i is the single-particle energy, t_{ij} are the so-called hopping integrals (all of them: t_0 (intramolecular) and t_1 , and t_2 (intermolecular) have been marked explicitly in Fig. 1), U is the on-site Coulomb repulsion, and K_{ij} is the amplitude of intersite Coulomb repulsion. The configuration of the molecules and related microscopic parameters are shown in Fig. 1. Explicitly, those parameters can be

* kadzielawa@th.if.uj.edu.pl

† andrzej.biborski@agh.edu.pl

‡ ufspalek@if.uj.edu.pl

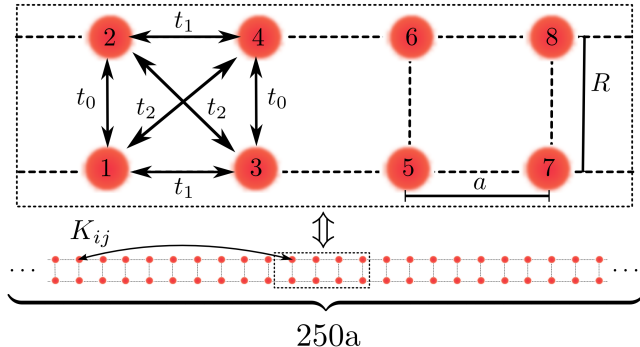


FIG. 1. Schematic representation of H_2 molecular chain with possible nearest-neighbor and next nearest neighbor hoppings $\{t_i\}_{i=0,1,2}$ marked. The labeling of the sites $i = 1, 2, 3, \dots$ is specified, as well as the bond length R at intermolecular distance a . The radius of included intersite Coulomb interaction is equal to $250a$ in the atomic representation. (see main text).

defined in the following manner

$$\begin{aligned} \langle w_i | H_1 | w_j \rangle &\equiv \int d^3r w_i^*(\mathbf{r}) H_1(\mathbf{r}) w_j(\mathbf{r}) \\ &\equiv \epsilon_i \delta_{ij} + t_{ij} (1 - \delta_{ij}), \end{aligned} \quad (2)$$

$$\begin{aligned} \langle w_i w_j | V_{12} | w_i w_j \rangle &\equiv \int d^3r d^3r' |w_i(\mathbf{r})|^2 V_{12}(\mathbf{r} - \mathbf{r}') |w_j(\mathbf{r}')|^2 \\ &\equiv U \delta_{ij} + K_{ij} (1 - \delta_{ij}), \end{aligned} \quad (3)$$

where H_1 is the Hamiltonian of single electron in the medium and V_{12} is the Coulomb repulsive interaction for a single pair of them. Furthermore, the Wannier functions are defined in terms of atomic (Slater) functions, i.e.,

$$w_i(\mathbf{r}) = \sum_j \beta_{ij} \psi_j(\mathbf{r}), \quad (4)$$

where the 1s-type Slater function is defined as $\psi_i(\mathbf{r}) \equiv \psi(\mathbf{r} - \mathbf{R}_i) = (\alpha^3/\pi)^{1/2} \exp(-\alpha|\mathbf{r} - \mathbf{R}_i|)$, with α being its inverse size in the medium, here taken as a variational parameter for given intermolecular distance a and determined in the correlated state ($i \equiv \mathbf{R}_i$ is the i -th proton position). Each Slater function is approximated by its expansion in the Gaussian basis

$$\psi_i(\mathbf{r}) \approx \alpha^{\frac{3}{2}} \sum_{q=1}^p B_q \left(\frac{2\Gamma_q^2}{\pi} \right)^{\frac{3}{4}} e^{-\alpha^2 \Gamma_q^2 |\mathbf{r} - \mathbf{R}_i|^2}, \quad (5)$$

with p being the number of Gaussian functions taken into account to express accurately the functions $\{\psi_i(\mathbf{r})\}$ and $\{B_q, \Gamma_q\}$ is the set of adjustable parameters obtained from a separate procedure (for details see [19]). In effect, all the parameters: ϵ_i , t_{ij} , U , K_{ij} can be expressed in terms of α and are determined in the correlated state (after the exact diagonalization in the Fock space has also been carried out simultaneously). Strictly speaking,

to obtain proper atomic limit we have to take: $\epsilon_i \rightarrow \epsilon_i^{eff} = \epsilon_i + (1/2) \sum_j (2/R_{ij} + K_{ij})$ [20].

A brief methodological note is in place here. We diagonalize exactly the clusters up to $n = 5$. However, to account for the long-range nature of Coulomb interactions, we include them in ϵ_i , t_{ij} , K_{ij} , and the ion-ion interaction up to the distance $250a$. In other words, we regard our cluster of nH_2 molecules as a single block of the length na immersed in the periodic system. In this manner, we utilize the periodic boundary conditions in the same sense as in the cluster perturbation approaches, cf. e.g. Ref. [21].

First, we determine values of hopping integrals t_0 , t_1 , and t_2 Hubbard (intraatomic) and intersite interactions U and K_{ij} , by determining the Wannier functions defining them. The Wannier functions are expressed in terms of (atomic) Slater functions of adjustable size α^{-1} , each of which is expressed in turn via $p = 9$ Gaussian functions [20]. In the next step, we determine the lowest eigenvalue of the Hamiltonian (1) with periodic boundary conditions, by diagonalizing it by means of Lanczos algorithm. By finding the ground state energy in the Fock space and subsequently, by optimizing the energy also with respect to the size α^{-1} , we obtain a true physical ground state energy in the correlated state for given intermolecular distance a . Such extended calculations make the results not limited to the parametrized-model considerations, as U , t_{ij} , and K_{ij} are evaluated explicitly, as is also the ground state energy, for fixed a . One should note that in the procedure the bond length is also optimized ($R \rightarrow R_{eff}$). All this is carried out first for the zero-applied force to obtain the system equilibrium configuration, i.e., the energy and the effective bond length R_{eff} in the multimolecular configuration. In the second step, we apply the external compressing force f to the end molecules and determine the enthalpy minimum to trace the system evolution as a function of a . The part of the procedure connected with the optimization of the single-particle wave functions has been discussed in detail elsewhere [20]. The code used for the computation is also available [22].

Typical numerical procedure starts with fixing a and R , and selecting input value for the variational parameter α . Next, we vary the inverse wave function size α to find the physical ground-state energy employing, at every step, the so-called *process-pool solution* for the computationally expensive problem of obtaining the microscopic parameters. We include all the intersite interactions for the sites with a relative distance smaller than $250a$. The accuracy of the numerical results is set to be of the order of $10^{-4} Ry$. Impact of these parameters was examined carefully in [20] and achieving the values above proved to be sufficient. The long range of the interactions in the atomic representation is expected to emulate correctly a longer-chain behavior.

3. Results In Fig. 2 we display the system enthalpy as a function of force f exerted on the molecules. We selected such anisotropic form of f , since a proper account

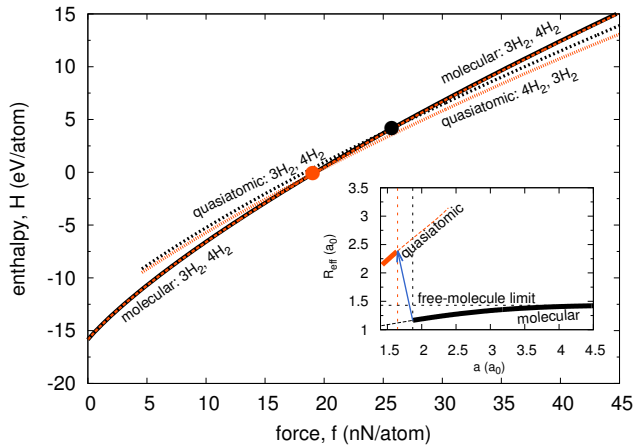


FIG. 2. Phase diagram encompassing quasiatomic and molecular states for nH_2 chain as a function of exerted force along the chain. Inset: Effective bond length R_{eff} vs. the intermolecular distance a .

of hydrostatic-pressure case would require a consideration of square or 3-dimensional clusters, so the all directions are physically equivalent. We assume a spatially homogeneous state of the system, in accordance with periodic boundary conditions. Typically, two solutions appear which we call respectively as the molecular and the quasi-atomic, each of which is characterized below. The solid points mark the transition points for $4H_2$ (left) and $3H_2$ (right). In the Inset we show the effective bond length R_{eff} vs a . Note two specific features. First, the lattice contracts in a discontinuous manner at the transition and second, the bond length jumps then from an almost single-molecule value $R_{eff} \ll a$ to the limit $R_{eff} \sim a$ signaling their separation into a quasi-atomic configuration. The last feature of the transition is explicitly illustrated in Fig. 3, where the projected electron density onto the plane composed of molecules is shown both on the molecular (top) and the quasi-atomic (bottom) sides of transition. The parameters a and R_{eff} are listed also in each case.

In Fig. 4 the interdependence of the intermolecular distance versus force is provided. As shown also in the inset to Fig. 2, this figure demonstrates the first-order transition, since the cell volume a changes discontinuously at this mol. \rightarrow quasiat. transition from $1.869a_0$ to $1.647a_0$. In the inset to Fig. 4 we provide the ratio of the Hubbard interaction U to the bandwidth defined as $W = -4t_1 + |t_0 + 2t_2| - |t_0 - 2t_2|$, as a function of f . Note the fundamental characteristic: this ratio jumps from the value $U/W \sim 1.49$ to 0.8 . So, the system is indeed strongly correlated at the transition with the effective gap near the transition from the molecular side estimated as $\epsilon_g/W = U/W - 1 \approx 0.49$. Furthermore, the value $U/W \sim 1$ is the typical value for the Mott-Hubbard transition, weakly dependent on the system structure [23]. It is also interesting to note that here the Mott-Hubbard transition takes place from a non-magnetic (spin-singlet)

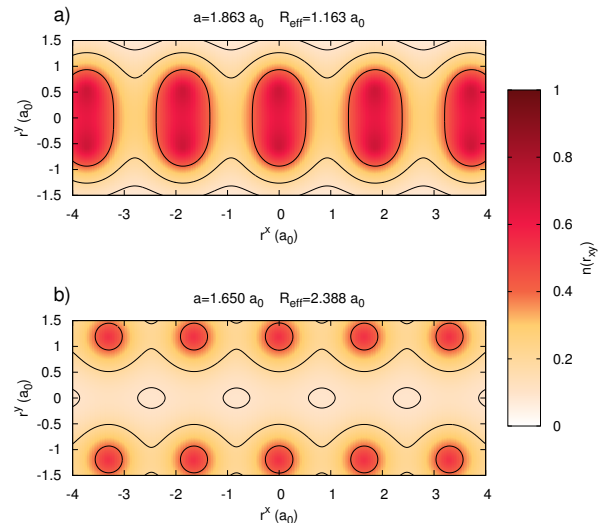


FIG. 3. Electron density projected onto the plane of H_2 molecules near the molecular \rightarrow atomic transition: a) for the molecular state; b) for the quasiatomic state. In case a) the density is very small in the space in between molecules (vertical line joining the atoms). The critical intermolecular distance a and the effective bond length R_{eff} are also specified in each of the states. The corresponding critical force is $f_C = 25.705nN$ for $3H_2$ system.

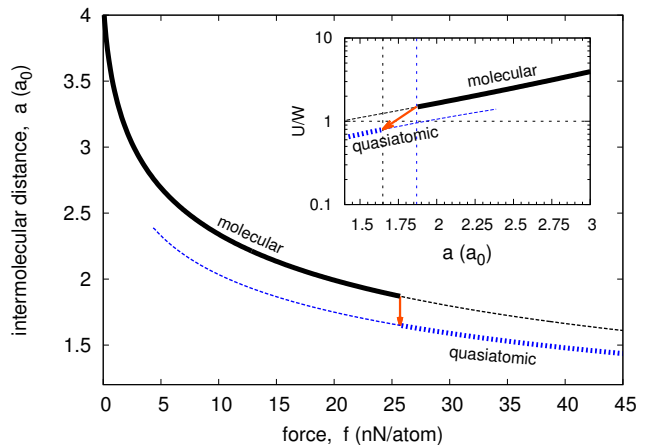


FIG. 4. Equilibrium intermolecular distance a versus exerted force f for the case of $3H_2$ system. The transition is of the first order as marked. Inset: U/W ratio vs. a showing that in the quasiatomic state $U/W \sim 0.8$ signaling the onset of a correlated metallic state.

molecular configuration to a correlated atomic solid, with strong suggestion for metallicity ($U/W < 1$) of such system with one electron per atom.

In Fig. 5 we present a dependence of the intramolecular (t_0) and intermolecular (t_1) hopping parameters. At the transition the parameters t_0 and t_1 roughly equalize showing again that the solid at small a is of quasi-atomic nature. In the inset we present the intramolecu-

TABLE I. Microscopic parameters at the molecular \rightarrow quasiatomic transition. The values are in eV if not specified otherwise.

	a (a_0)	R (a_0)	W	t_0	t_1	t_2	U	K_0	K_1	K_2	$\alpha(a_0^{-1})$
molecular	1.869	1.164	17.881	-15.487	-6.161	1.691	26.472	15.238	13.516	10.551	1.194
quasiatomic	1.647	2.386	33.124	-5.270	-8.445	0.164	26.404	10.825	14.701	8.976	1.251

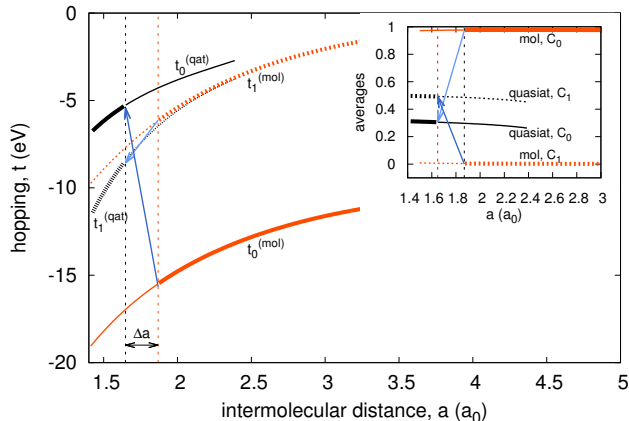


FIG. 5. Evolution of the intra- and inter-molecular hopping parameters, t_0 and t_1 respectively, versus intermolecular distance a . Note the jump of a at the transition molecular \rightarrow quasiatomic configurations as marked by the arrows. Inset: hopping probabilities: intra- and inter-molecular, C_0 and C_1 , respectively. For discussion see main text.

lar ($C_0 \equiv \langle \hat{c}_{1\sigma}^\dagger \hat{c}_{2\sigma} \rangle$) and intermolecular ($C_1 \equiv \langle \hat{c}_{1\sigma}^\dagger \hat{c}_{3\sigma} \rangle$) hopping probabilities. In the molecular state $C_0 \approx 1$ and $C_1 \approx 0$ (a strong molecular bond is formed), whereas in the quasiatomic state $C_0 \sim C_1$. These two quantities illustrate thus in a direct manner the nature of the states and in particular, the bonding in the quasiatomic solid state. For the sake of completeness, in Table I we list all the principal microscopic parameters in the correlated state for intermolecular distances at transition. The values of K_{ij} converge towards the asymptotic value $K_{ij} \rightarrow 0$ slowly. Such behavior is in accordance with the view [24] that the long-range part of the Coulomb interaction is not screened efficiently in low-dimensional systems. This is the reason why we have taken their long-range character. Parenthetically, note that we have neglected the direct exchange interaction and the so-called correlated-hopping terms [25], as they are of much smaller amplitude at these distances. Note also that the Mott criterion at the transition [26, 27] takes in the present situation the form $a_B n_C^{1/d} \equiv (\alpha a)^{-1} \approx 0.45$ at the transition, not too far from the value 0.25 for 3-dimensional ($d = 3$) systems.

4. Outlook We have described in a rigorous manner the behavior of electrons in the short H_2 chains connected via the Coulomb interaction with the further molecules, as well as utilizing the periodic boundary conditions, emulating together an extended-chain behavior. Amazingly,

the results obtained meet some of the features one can expect for a three-dimensional hydrogen molecular \rightarrow quasiatomic transformation. Obviously, no detailed realistic phase diagram can be obtained, as both the structural details and the effect of zero-point motion are still missing. However, a unique connection to the Mott-Hubbard transition is established. A direct proof of metallicity of the quasiatomic state would involve the determination of optical conductivity [28]. The model formulated here may form a basis for quantitative approach to solid hydrogen with a proper account of electronic correlations. In such approach a three-dimensional realistic model must be constructed. We think that tackling of this problem is possible on a small scale within our **Exact Diagonalization Ab Initio** (EDABI) approach employed here and to other problems [29] involving electronic correlations as an essential aspect of their physical properties. For 3d system, approximate second-quantization diagonalization schemes such as the statistically-consistent Gutzwiller approximation may be used with concomitant single-particle wave-function optimization [27]. These methods can be tested in the present exact limit.

One should also note that the principal assumption made at this point is that the protons form a lattice even in the atomic phase, not a proton-electron quantum-liquid plasma [16, 30–32]. Such problem is possible to tackle within the present model by assessing the optimal ground-state energy for a random choice of the proton positions. But first, an accurate estimate of the zero-point motion amplitude and the corresponding energy [14] must be carried out for an extended system with correlations [33].

Computer animation of the molecular \rightarrow quasiatomic transition is attached as Supplemental material [34].

5. Methodological remark The correlated ladder systems modeled by the (extended) Hubbard model have been studied extensively in the past (cf. e.g. [35]). Those studies differ from the problem discussed here. We start with the physical H_2 spin-singlet-insulator chain. Under pressure, the spin-singlet states transform into a quasiatomic correlated state. Most importantly, we treat the correlations within the cluster of n molecules rigorously and at each step determine the ladder rung size (bond length R) and the equilibrium lattice constant a . Such analysis has not been carried out so far and provides also the values of the microscopic parameters.

6. Acknowledgments We are grateful to Drs. Adam Rycerz and Marcello Acquarone, and to Prof. Maciej M. Maška for helpful discussions. The work was supported by the National Science Centre (NCN), Grant No. DEC-2012/04/A/ST3/00342.

- [1] E. Wigner and H. B. Huntington, "On the Possibility of a Metallic Modification of Hydrogen," *J. Chem. Phys.* **3**, 764 (1935).
- [2] H. K. Mao and R. J. Hemley, "Ultrahigh-pressure transitions in solid hydrogen," *Rev. Mod. Phys.* **66**, 671 (1994).
- [3] I. Silvera, "The insulator-metal transition in hydrogen," *Proc. Natl. Acad. Sci. U.S.A.* **107**, 12743 (2010).
- [4] J. M. McMahon, M. A. Morales, C. Pierleoni, and D. M. Ceperley, "The properties of hydrogen and helium under extreme conditions," *Rev. Mod. Phys.* **84**, 1607–1653 (2012).
- [5] I. Baraffe, G. Chabrier, and T. Barman, "The physical properties of extra-solar planets," *Rep. Prog. Phys.* **73**, 016901 (2010).
- [6] W. Kołos and L. Wolniewicz, "Improved theoretical ground-state energy of the hydrogen molecule," *J. Chem. Phys.* **49**, 404 (1968).
- [7] A. E. Curzon and A. J. Mascall, "The crystal structures of solid hydrogen and solid deuterium in thin films," *British Journal of Applied Physics* **16**, 1301 (1965).
- [8] R. T. Howie, Ch. L. Guillaume, T. Scheler, A. F. Goncharov, and E. Gregoryanz, "Mixed Molecular and Atomic Phase of Dense Hydrogen," *Phys. Rev. Lett.* **108**, 125501 (2012).
- [9] F. Gebhard, *The Mott Metal-Insulator Transition: Models and Methods* (Springer, Berlin, 1997).
- [10] A. P. Kądziaława, J. Spałek, J. Kurzyk, and W. Wójcik, "Extended Hubbard model with renormalized Wannier wave functions in the correlated state III," *Eur. Phys. J. B* **86**, 252 (2013).
- [11] N. W. Ashcroft, "Metallic Hydrogen: A High-Temperature Superconductor?" *Phys. Rev. Lett.* **21**, 1748–1749 (1968).
- [12] E. Babaev, A. Sudbo, and N. W. Ashcroft, "A superconductor to superfluid phase transition in liquid metallic hydrogen," *Nature* **431**, 668 (2004).
- [13] J. Kaczmarczyk, J. Spałek, T. Schickling, and J. Büne-mann, "Superconductivity in the two-dimensional Hubbard model: Gutzwiller wave function solution," *Phys. Rev. B* **88**, 115127 (2013).
- [14] A. Kądziaława, A. Bielas, M. Acquarone, A. Biborski, M. M. Maška, and J. Spałek, " H_2 and $(H_2)_2$ molecules with an ab initio optimization of wave functions in correlated state: electron-proton couplings and intermolecular microscopic parameters," *New J. Phys.* **16**, 123022 (2014).
- [15] S. Azadi, W. M. C. Foulkes, and T. D. Kühne, "Quantum Monte Carlo study of high pressure solid molecular hydrogen," *New J. Phys.* **15**, 113005 (2013).
- [16] G. Mazzola, S. Yunoki, and S. Sorella, "Unexpectedly high pressure for molecular dissociation in liquid hydrogen by electronic simulation," *Nat. Commun.* **5**, 3487 (2014).
- [17] I. Errea, M. Calandra, Ch. J. Pickard, J. Nelson, R. J. Needs, Y. Li, H. Liu, Y. Zhang, Y. Ma, and F. Mauri, "High-Pressure Hydrogen Sulfide from First Principles: A Strongly Anharmonic Phonon-Mediated Superconductor," *Phys. Rev. Lett.* **114**, 157004 (2015).
- [18] S. Azadi and W. M. C. Foulkes, "Fate of density functional theory in the study of high-pressure solid hydrogen," *Phys. Rev. B* **88**, 014115 (2013).
- [19] A. Rycerz, *Physical properties and quantum phase transitions in strongly correlated electron systems from a combined exact diagonalization - ab initio approach*, Ph.D. thesis, Jagiellonian University (2003), [th-www.if.uj.edu.pl/ztnms/download/phdTheses/Adam_Rycerz_doktorat.pdf](http://www.if.uj.edu.pl/ztnms/download/phdTheses/Adam_Rycerz_doktorat.pdf).
- [20] A. Biborski, A. P. Kądziaława, and J. Spałek, "Combined shared and distributed memory ab-initio computations of molecular-hydrogen systems in the correlated state: process pool solution and two-level parallelism," *Comp. Phys. Commun.* (in press) (2015).
- [21] Maciej M. Maška, "Ground-state energy of the Hubbard model: Cluster-perturbative results," *Phys. Rev. B* **57**, 8755 (1998).
- [22] A. Biborski and A. Kądziaława, "QMT: Quantum Metallization Tools Library," (2014), <https://bitbucket.org/azja/qmt>.
- [23] A. Datta, J. M. Honig, and J. Spałek, "Discontinuous metal-insulator transitions of correlated electrons at nonzero temperature: Effect of the shape of the density of states," *Phys. Rev. B* **44**, 8459–8466 (1991).
- [24] J. Hubbard, "Generalized Wigner lattices in one dimension and some applications to tetracyanoquinodimethane (TCNQ) salts," *Phys. Rev. B* **17**, 494 (1978).
- [25] J. Spałek, R. Podsiadły, W. Wójcik, and A. Rycerz, "Optimization of single-particle basis for exactly soluble models of correlated electrons," *Phys. Rev. B* **61**, 15676 (2000).
- [26] N. F. Mott, *Metal-insulator transitions* (Taylor & Francis, London, 1991).
- [27] J. Spałek, J. Kurzyk, R. Podsiadły, and W. Wójcik, "Extended Hubbard model with the renormalized Wannier wave functions in the correlated state II: quantum critical scaling of the wave function near the Mott-Hubbard transition," *Eur. Phys. J. B* **74**, 63 (2010).
- [28] M. J. Rozenberg, G. Kotliar, H. Kajueter, G. A. Thomas, D. H. Rapkine, J. M. Honig, and P. Metcalf, "Optical Conductivity in Mott-Hubbard Systems," *Phys. Rev. Lett.* **75**, 105–108 (1995).
- [29] J. Spałek, E.M. Görlich, A. Rycerz, and R. Zahorbeński, "The combined exact diagonalization-ab initio approach and its application to correlated electronic states and Mott-Hubbard localization in nanoscopic systems," *J. Phys.: Condens. Matter* **19**, 255212 (2007), pp. 1-43.
- [30] M. A. Morales, C. Pierleoni, E. Schwegler, and D. M. Ceperley, "Evidence for a first-order liquid-liquid transition in high-pressure hydrogen from ab initio simulations," *Proc. Natl. Acad. Sci. U.S.A.* **107**, 12799 (2010).
- [31] S. A. Bonev, E. Schwegler, T. Ogitsu, and G. Galli, "A quantum fluid of metallic hydrogen suggested by first-principles calculations," *Nature* **431**, 672 (2004).
- [32] W.J. Nellis, "Discovery of Metallic Fluid Hydrogen at 140 GPa and Ten-fold Compressed Liquid Density," *The Review of High Pressure Science and Technology* **17**, 328–333 (2007).
- [33] J. Spałek and A. Rycerz, "Electron localization in a one-dimensional nanoscopic system: A combined exact diagonalization - an ab initio approach," *Phys. Rev. B* **64**, 161105(R) (2001).
- [34] See Supplemental Material at [] for computer animation of molecular \rightarrow quasiautomatic transition.

- [35] M. Tsuchiizu and A. Furusaki, “Generalized two-leg Hubbard ladder at half filling: Phase diagram and quantum criticalities,” *Phys. Rev. B* **66**, 245106 (2002).